
OPTION VALUATION THROUGH DEEP LEARNING OF TRANSITION PROBABILITY DENSITY

Haozhe Su

Nottingham Business School
Nottingham Trent University
Nottingham NG1 4FQ, UK
Haozhe.Su@ntu.ac.uk

M.V. Tretyakov

School of Mathematical Sciences
University of Nottingham
Nottingham NG7 2RD, UK
Michael.Tretyakov@nottingham.ac.uk

David P. Newton

School of Management
University of Bath
Bath BA2 7AY, UK
dpn25@bath.ac.uk

August 23, 2021

ABSTRACT

Transition probability densities are fundamental to option pricing. Advancing recent work in deep learning, we develop novel transition density function generators through solving backward Kolmogorov equations in parametric space for cumulative probability functions, using neural networks to obtain accurate approximations of transition probability densities, creating ultra-fast transition density function generators offline that can be trained for any underlying. These are “single solve”, so they do not require recalculation when parameters are changed (e.g. recalibration of volatility) and are portable to other option pricing setups as well as to less powerful computers, where they can be accessed as quickly as closed-form solutions. We demonstrate the range of application for one-dimensional cases, exemplified by the Black-Scholes-Merton model, two-dimensional cases, exemplified by the Heston process, and finally for a modified Heston model with time-dependent parameters that has no closed-form solution.

Keywords deep learning · option pricing · transition probability density · parametric PDEs · QUAD

1 Introduction

The use of deep learning in option pricing has a long history, dating back at least as far as the early 1990s (see, e.g., Malliaris & Salchenberger 1993; Hutchinson, Lo & Poggio 1994) and has built a large technical literature of applications and improvements aimed at creating more reliable setups linking underlying data directly with option prices in the markets and in calibrating implied volatilities. We do not review that literature since this is not the approach we take. Instead, we apply deep learning to replace the transition probability density calculations in option pricing models. The difficulties in extracting densities from market data are considerable, particularly in the tails (Figlewski 2009, 2018) but again that is not our aim. Rather, we use deep learning in place of other mathematical techniques in the calculation of transition density functions, training artificial neural networks using simulated data. A novel advance in our approach is in the parametric solution of partial differential equations (PDEs). It is usual in option pricing to solve a PDE for fixed parameters and to have to recalculate when changes are made, but here we create an engine that does not require us to solve the PDE again. This opportunity to change and considerably improve option valuation arises from recent advances in deep learning, as we will explain later when we show how to adapt and incorporate deep learning into the options calculations.

We demonstrate this new tool in option pricing by targeting for improvement numerical techniques under the umbrella term QUAD that directly use single- or multi-variable transition density functions. The considerable advances in deep learning capability since the introduction of approximations of the transition density function into the QUAD technique by Chen, Härkönen & Newton (2014) mean that deep learning now moves up to become a method of choice for inclusion into option pricing techniques using the transition density function.

Some of the fastest numerical option pricing methods with wide application to the combination of different option types and varied models for underlyings are in the QUAD family. The first paper in a series establishing the method (Andricopoulos et al. 2003) calculates option prices through integrating the product of the payoff function and the transition probability density function. This approach delivers results orders of magnitude faster than the other main techniques in derivatives pricing (tree methods, finite difference and Monte Carlo) because it does not require massive calculation between the key points in time that specify the option type (the boundary conditions). That first paper laid out the basic technique and demonstrated its use with plain vanilla European and American options, discrete barrier options, multiply-compounded options, Bermudans, changing strike prices, dividend adjustments, lookbacks and lookbacks with multiple underlyings. A second paper (Andricopoulos, Widdicks, Newton & Duck 2007) extended the method to options on multiple underlying assets, Parisian, Asian, ParAsians, multiple underlyings for Bermudan as well as American (with dividends) and barrier options up to 5 underlyings. This established QUAD as a universal technique for underlying processes ranging from Black-Scholes-Merton (Black & Scholes 1973; Merton 1973) to jump-diffusion (Merton 1976) and to certain interest rate models such as those of Vasicek (1977) and Cox, Ingersoll Jr & Ross (1985). Others can be found elsewhere; for example, Heston (1993) combined with Merton jump-diffusion (1976) is demonstrated by Su, Chen & Newton (2017). Applications in the QUAD stable of techniques include the method of recursive projections by Cosma, Galluccio, Pederzoli & Scaillet (2020) investigating investor suboptimal non-exercise of short maturity American call options on dividend-paying stocks, modelling the underlying via the Heston model with jumps.

Nevertheless, lack of transition densities limited the range of underlying processes that could be tackled by quadrature methods for derivatives pricing. A third paper (Chen et al. 2014) finessed this through insertion of interchangeable approximation techniques. This advanced the method further towards the universality promised by Andricopoulos et al. (2003) and Andricopoulos et al. (2007), in a particularly satisfying mathematical manner, so as to become a framework for a wider set of underlying processes including CEV (Cox 1996) and quadratic local volatility, an expanded the range of interest rate models, and stochastic volatility models with early exercise, demonstrated for the Heston (1993) and SABR models (Hagan, Kumar, Lesniewski & Woodward 2002). This idea opened a new door for the method and works well but, as noted in the paper, a limitation is the accuracy of the transition probability density approximation engines. This leads to a computational bottleneck for the more practically interesting models of the underlying. We may either try to find a better approximation technique (not a straightforward task) or, as we propose in the present paper, go in a new direction with deep learning incorporated as a different engine. This not only removes the bottleneck in speed that comes with the approximations but, more significantly, the deep learning route innovates by being “single solve”, as we shall show, and applicable across all option pricing techniques using the transition density function.

It is only in rare cases that we are able to find the transition probability density functions in closed form; i.e. we have an exact formula which does not require numerical methods to calculate the transition probability density. The well-known Black-Scholes-Merton model is one such with a closed form solution. Sometimes, we are able to obtain a semi-closed form solution for the transition probability density. These cases require additional calculations such as use of Bessel functions or calculations in the complex plane. For example, the CEV process suggested by Cox (1996) has a semi-closed form solution (see, e.g., Chen et al. 2014). Lewis (2016) reduces the semi-closed form of the joint transition density for Heston’s (1993) stochastic volatility process and the 3/2-stochastic volatility process, a variation of the Heston process (Heston 1997; Lewis 2016). In certain cases, transition probability densities are not known in closed form but their characteristic functions are. Densities can subsequently be calculated using inverse Fourier transform (O’Sullivan 2005; Lord et al. 2008; Su et al. 2017). For the majority of underlying processes, where we have no other ways to calculate density, we can turn to density approximations, as shown by Chen et al. (2014). For example, Ait-Sahalia (2002), Ait-Sahalia (2008), Henry-Labordère (2008) and Filipović et al. (2013) provide approximations to the density of various underlying processes. However, density approximations do have limitations. One is that they cannot universally provide approximations of all the underlying processes. For example, the approximation techniques used in Chen et al. (2014) cannot solve for jump-diffusion processes and the density approximation is only accurate when the time step is very small. On top of this, density approximations can be cumbersome and may require complex computations. Thus, universality for the underlying is available for those willing to put in the necessary effort but its practicality is more limited than we would wish. It is true that conventional numerical methods, particularly finite differences, can also be used to solve for density (see, e.g., Hagan et al. 2014; Floc’h & Kennedy 2014; Su & Newton 2020) but they are computationally expensive. More importantly, these only allow calculation for a single set of

parameters of an underlying process at a time, so they are far from ideal. A faster and more generic way of calculating density is needed for practical universal application. This leads us to deep learning.

Deep learning has an even longer history outside option pricing, having been developed since the 1940s and undergone several name changes until its current guise from 2006 (Goodfellow, Bengio & Courville 2016), following an advance in neural networks by Hinton, Osindero & Teh (2006). Key contributors to the surge in applicability of deep learning in areas outside finance are massive increases in available digitised data together with networking of computers (“Big Data”) and far greater computing power, not only in central processing units (CPUs) but especially in graphics processing units (GPUs) together with improved software. Helpful results from these developments are the readily-available techniques and neural network infrastructure developed by the machine learning and deep learning community worldwide, and the alternative of using cloud computing resources through the internet.

Deep learning algorithms offer an effective way of solving ordinary differential equations and PDEs. Prototypes of algorithms as differential equation solvers may be found in work by Lee & Kang (1990) and Dissanayake & Phan-Thien (1994). Subsequently, similar feedforward approaches have been introduced by van Milligen et al. (1995), Lagaris et al. (1998) and Lagaris et al. (2000). Schmidhuber (2015) and Yadav et al. (2015) review the area. Calculations are very fast once the learning networks are trained but they suffer the drawback of needing to sample the data using a mesh. Mesh-free approaches to solving PDE problems based on deep learning are presented by Sirignano & Spiliopoulos (2018) - see also Rackauckas et al. (2020) and references therein. Here, we adapt the “Deep Galerkin Method” (DGM) deep learning algorithm developed by Sirignano and Spiliopoulos for computing densities of underlying processes. Through this algorithm we arrive at an approximate PDE solution represented by a deep neural network, which is trained to satisfy the differential operator, initial condition, and boundary conditions.

The key for this work is that deep learning algorithms for PDEs can be extended to parametric PDE problems (see, e.g., Kutyniok et al. 2019, Geist et al. 2020, Khoo et al. 2017). By parametric problems, we understand that we are interested not just in solving a PDE in a domain of its independent variables (time and space) as standard PDE solvers do, but also in having a representation of a PDE’s solution for a range of its parameters’ values. There are several types of methods under the umbrella of model order reduction capable of dealing with parametric PDE problems (see, e.g., Antoulas et al. 2015 and references therein). The type used in this paper, based on deep learning networks, has been shown over recent years to be very robust and universal (see, e.g., Kutyniok et al. 2019, Geist et al. 2020, Khoo et al. 2017 and references therein, and also its use in this paper). Parametric PDE problems arise naturally in finance. Indeed, in finance applications we need to be able to find option prices, densities for the underlying price process, etc. not only as functions of spot and maturity but also as functions of volatility and other parameters of the underlying process to satisfy the practical need for frequent recalibration of models. Frequent recalibration imposes the requirement for valuations to be very fast for a range of the parameters’ values. Deep learning applied to parametric PDE problems can achieve this, as we shall demonstrate. We emphasise that standard PDE solvers (e.g. finite differences) give approximations of PDE solutions only for given, fixed values of parameters and need to be run online each time a parameter changes, making them uncompetitive for the parametric problem described above. An important feature of the use of deep learning for solving parametric problems as applied to option pricing problems is that it is “single solve” such that, once trained, the algorithm delivers results for any set of parameters without the need to re-run calculations. In the spirit of the QUAD papers, this is a new “engine” offering a superior alternative to previous approaches ensuring that the method is not only of universal application but also retains its high speed across all models for the underlying.

These advantages are the prize. Nevertheless, formulating the use of deep learning techniques to calculate transition probability densities is a challenge. We know that the solution of the Fokker-Planck (Kolmogorov forward) equation is the transition probability density. Its initial condition is a Dirac delta function, which has zero value everywhere except at one point where it is infinite. Appearance of the delta function in the initial condition makes it impractical to use DGM for the Fokker-Planck equation. Al-Arabi et al. (2018) make an attempt to solve the Fokker-Planck equation for the Ornstein-Uhlenbeck process by assuming a Gaussian initial condition. Pleasing as this is, it is rather inefficient and cannot be generalised to other underlying processes simply because other processes do not possess Gaussian shapes. Here, we circumvent this difficulty by considering instead the backward Kolmogorov equation with terminal condition being a step function, whose solution is the cumulative distribution function. As in Sirignano & Spiliopoulos (2018), we base our deep neural network, used for solving the parametric problem for the backward Kolmogorov equation, on a variant of the widely used Long Short-Term Memory networks (LSTMs) of Hochreiter & Schmidhuber (1997).

In summary, we approximate the cumulative distribution function then calculate density using numerical differentiation via deep learning. Once it is trained, a deep learning network can be accessed very quickly - as quickly as calculating closed-form solutions. We are the first in the literature using a deep learning approach to solve this problem successfully. In the following sections, we benchmark our approach on the geometrical Brownian motion and the Heston model, for which there are analytical expressions for transition densities. We also demonstrate benefits of our approach on a more complicated Heston model with time-dependent coefficients.

2 Methods

We set the scene by expressing option prices via transition probability density functions (TPDFs) of the underliers. For clarity of exposition, we use a simple one-dimensional model. In Section 2.2, we show how to formulate PDE problems for solving to find TPDFs. In Section 2.2.2, we show how to apply deep learning techniques to approximating parametric PDEs and using this to solve backward Kolmogorov equations in order to find parametric TPDFs in a computationally effective manner.

2.1 Option pricing via the transition density of an underlier

Before moving on to financially more interesting cases, let us consider the simplest model where a single underlying, $S(t)$, follows a stochastic differential equation (SDE) written under the forward measure:

$$dS = \sigma(t, S)dW, \quad S(0) = S_0. \quad (1)$$

Here, $W(t)$ is a one-dimensional standard Wiener process and the volatility $\sigma(t, x)$ is a deterministic function. For example, the famous Black-Scholes-Merton option pricing formula rests on the model in which the asset's price follows geometric Brownian motion:

$$dS = \sigma S dW, \quad S(0) = S_0. \quad (2)$$

The European option price $V(0, S_0)$ at time $t = 0$ on an underlying $S_{0, S_0}(t)$ with the spot price $S_{0, S_0}(0) = S_0$ and with a payoff function $f(x)$ and maturity T is expressed by

$$V(0, S_0) = E[f(S_{0, S_0}(T))]. \quad (3)$$

Since the solution of SDE (1) is a Markov process, we can write

$$V(0, S_0) = \int_0^{+\infty} f(y)p(0, S_0; T, y)dy, \quad (4)$$

where $p(t, S_0; T, y)$ is the TPDF for the solution $S_{t, S_0}(T)$ of (1) from (t, S_0) to (T, y) .

Computationally, instead of working in the asset price space, it is preferable to use the log-asset price space since this change of variables allows us to stretch the phase space, i.e., the left bound of the integration becomes $-\infty$. This change of variables is important for training an artificial neural network for the backward Kolmogorov equation, as we will discuss later (see Section 2.2.2); making use of log-asset price improves accuracy of neural network training. By Ito's formula, we obtain the SDE in the log-space, i.e. for $X(t) = \ln S(t)$:

$$dX = -\frac{1}{2}\sigma^2(t, e^{X(t)})dt + \sigma(t, e^{X(t)})dW, \quad X(0) = x_0. \quad (5)$$

Letting $x_0 = \ln S_0$, (4) becomes

$$V(0, S_0) = \int_{-\infty}^{+\infty} f(e^y)p(0, x_0; T, y)dy, \quad (6)$$

where $p(t, x; T, y)$ is the TPDF for the solution $X_{t, x}(T)$ of the SDE (5) from (t, x) to (T, y) . Since the transition starts from time 0, we will use the simpler notation $p(x; s, y)$ or in short $p(s, y)$ instead of $p(0, x; s, y)$.

Thus, in Eq. (6), if we know the TPDF $p(t, x; T, y)$, we can readily calculate the price of the option, $V(0, S_0)$. To this end, the integral in Eq. (6) can be approximated via quadrature after appropriate truncation of the integration range $[-\infty, +\infty]$. Details of QUAD implementation for a given density can be found in the earlier papers (Andricopoulos et al. 2003, 2007).

2.2 Preliminaries on transition densities

In the previous subsection we highlighted the importance of the TPDF of the underlying asset price process in option pricing. It is straightforward to write the Fokker-Planck (forward Kolmogorov) PDE for a TPDF. However, its initial condition contains the Dirac delta function which hinders effective application of numerical techniques including the deep learning approach we present in this paper. We circumvent this problem by proposing a novel approach through solving the backward Kolmogorov PDE for the cumulative distribution function (CDF) and differentiating it to obtain the TPDF.

2.2.1 The forward equation for transition density

The Fokker-Planck (forward Kolmogorov) equation governs the time evolution of the transition probability for SDEs' solutions (Gichman & Skorochod 1972, Freidlin 1985, Gardiner 2004). In the case of the SDE (5), it takes the form

$$\frac{\partial}{\partial s} p(s, y) = \frac{1}{2} \frac{\partial^2}{\partial y^2} [\sigma^2(s, e^y) p(s, y)] + \frac{1}{2} \frac{\partial}{\partial y} [\sigma^2(s, e^y) p(s, y)], \quad s > 0, y \in \mathbb{R}, \quad (7)$$

with initial condition for a fixed x

$$p(0, y) = \delta(y - x), \quad y \in \mathbb{R}, \quad (8)$$

where $\delta(\cdot)$ is the Dirac delta function. Recall that the full notation for the TPDF is $p(s, y) = p(0, x; s, y)$. Note that the PDE problem Eqs. (7)-(8) is with respect to the variables (s, y) while x is a parameter. We recall that the Dirac delta function $\delta(y - x)$ is a function with zero value everywhere except at x :

$$\delta(y - x) = \begin{cases} +\infty, & y = x, \\ 0, & y \neq x, \end{cases} \quad (9)$$

and $\int_{-\infty}^{+\infty} \delta(y - x) dy = 1$. Because the function is infinite at the point $y = x$, it is difficult to solve the problem (7)-(8) numerically. This limitation extends to approximation via the deep learning approach. Since it is tricky to solve the problem (7)-(8) for density, we need a smarter way to deal with this. Instead of solving for transition density directly, we first solve for the CDF and then use the CDF to calculate the TPDF. This method, as we will show later, is efficient in dealing with evaluating TPDFs.

2.2.2 The backward Kolmogorov equation for cumulative distribution function

We define the CDF of the log-stock price process $X_{t,x}(T)$ at terminal time T and the starting point (t, x) as

$$C(t, x; T, y) := \text{Prob}(X_{t,x}(T) \leq y) = \int_{-\infty}^y p(t, x; T, z) dz \quad (10)$$

where $\text{Prob}(X_{t,x}(T) \leq y)$ is the probability of the random variable $X_{t,x}(T)$ to be not greater than y .

In the case of the SDE (5), the function $C(t, x) = C(t, x; T, y)$ satisfies the backward Kolmogorov equation (see, e.g. Gichman & Skorochod 1972, Freidlin 1985, Gardiner 2004):

$$\frac{\partial}{\partial t} C(t, x) + \frac{1}{2} \sigma^2(t, e^x) \frac{\partial^2}{\partial x^2} C(t, x) - \frac{1}{2} \sigma^2(t, e^x) \frac{\partial}{\partial x} C(t, x) = 0, \quad t \in [0, T], \quad x \in \mathbb{R}, \quad (11)$$

with the terminal condition for a fixed y

$$C(T, x) = \mathbb{1}(x \leq y) = \begin{cases} 1, & x \leq y, \\ 0, & x > y, \end{cases}, \quad x \in \mathbb{R}. \quad (12)$$

We note that the problem (11)-(12) is written with negative direction of time, while the Fokker-Planck equation (7) has positive direction of time. The PDE problem (11)-(12) is with respect to the variables (t, x) and T and y are parameters. It is easier to solve numerically Eqs. (11)-(12) than Eqs. (7)-(8) since the terminal condition (12) contains the bounded function.

Using a deep learning artificial neural network, we approximate $C(t, x; T, y)$ and then, using an automatic differentiation built-in function from a deep learning library such as TensorFlow or finite differences, we evaluate the transition probability density $p(t, x; T, y)$ by differentiating $C(t, x; T, y)$ with respect to y ; that is

$$p(t, x; T, y) = \frac{\partial}{\partial y} C(t, x; T, y). \quad (13)$$

For most models of practical interest, the CDF $C(t, x; T, y)$ is a smooth function for $t < T$, hence the differentiation in Eq. (13) is well defined. Consequently, numerical differentiation of an approximate $C(t, x; T, y)$ can be done accurately. We discuss this in more detail in Section 3.

We note that the solution to the problem (11)-(12) depends not only on the independent variables (t, x) but also on the set of parameters, namely T, y and the volatility $\sigma(t, x)$, which can be parametrically encoded. A universal pricing engine requires a black box which can quickly and sufficiently accurately produce the TPDF for a range of values of the parameters so that we do not need to solve a PDE again e.g. after recalibration of the volatility. This leads us to the need to solve a parametric PDE problem, not just for a fixed values of parameters (and variable (t, x)) but for a set of them. Traditional numerical methods (finite difference, finite element, Monte Carlo, etc.) are designed to solve PDE problems with fixed parameters. In contrast, model order reduction methods for PDEs (Antoulas et al. 2015), and the most modern and universal of them, based on deep learning (Khoo et al. 2017, Kutyniok et al. 2019, Geist et al. 2020), are aimed at parametric PDE problems.

2.3 Deep learning as a PDE solver

Recent developments in deep learning allow us to effectively solve parametric PDE problems. Our implementation could be adapted to various neural networks; however, in this paper, we build our neural network following the Deep Galerkin Method (DGM) recently proposed by Sirignano & Spiliopoulos (2018) and we find its architecture effective in solving our problem. Next, we describe the DGM and how we adapt the method for solving parametric PDE problems.

2.3.1 Constructing the loss function

We start with a formal description of DGM used to solve a PDE problem under fixed parameters, which is later extended to solving a parametric PDE problem and illustrated on three finance examples. Let a domain $G \subset \mathbb{R}^d$ with the boundary ∂G and \mathcal{L} be an elliptic operator. Consider the parabolic PDE

$$\frac{\partial}{\partial t}u(t, \mathbf{x}) + \mathcal{L}u(t, \mathbf{x}) = 0, \quad (t, \mathbf{x}) \in [0, T] \times G, \quad (14)$$

with terminal condition

$$u(T, \mathbf{x}) = u_T(\mathbf{x}), \quad \mathbf{x} \in G, \quad (15)$$

and boundary condition

$$u(t, \mathbf{x}) = g(t, \mathbf{x}), \quad (t, \mathbf{x}) \in [0, T] \times \partial G. \quad (16)$$

We assume that this problem has a classical solution $u(t, \mathbf{x})$ (see e.g. Ladyzhenskaya et al. 1968).

We note that Eqs. (11)-(12) are of the form Eqs. (14)-(15) and that the backward Kolmogorov equation for any SDE has this form (see further examples in Sections 3-5).

Next, we would like to use deep learning algorithms to “learn” the function $u(t, \mathbf{x})$, which is an approximation of the solution to the PDE problem (14)-(15). In other words, we wish to train a deep neural network $f(t, \mathbf{x}; \boldsymbol{\theta})$ to approximate $u(t, \mathbf{x})$, where $\boldsymbol{\theta}$ are the trainable parameters of the neural network.

In order to train the network, we need to construct the loss function $L(f)$ as

$$L_1(f) = \left\| \frac{\partial}{\partial t}f(t, \mathbf{x}; \boldsymbol{\theta}) + \mathcal{L}f(t, \mathbf{x}; \boldsymbol{\theta}) \right\|_{[0, T] \times G, \nu_1}^2, \quad (17)$$

$$L_2(f) = \|f(T, \mathbf{x}; \boldsymbol{\theta}) - u_T(\mathbf{x})\|_{G, \nu_2}^2, \quad (18)$$

$$L(f) = \lambda L_1(f) + L_2(f), \quad (19)$$

where $L_1(f)$ is a loss in the differential operator term (the residual), and $L_2(f)$ is loss in the terminal condition term. Here $\|f(y)\|_{\mathcal{Y}, \nu}^2$ is the weighted L^2 -norm defined as $\|f(y)\|_{\mathcal{Y}, \nu}^2 = \int_{\mathcal{Y}} |f(y)|^2 \nu(y) dy$, where $\nu(y)$ is a positive probability density on a domain \mathcal{Y} . In the context of this paper’s application, we choose $\nu_1(y)$ as the probability density for uniform distribution on the time-price domain $\mathcal{Y} = [0, T] \times G$ and $\nu_2(y)$ as the probability density for uniform distribution on the price domain $\mathcal{Y} = G$.

Our loss function (19) has two differences compared with the loss function of the original DGM of Sirignano & Spiliopoulos (2018). First, we have a new hyperparameter λ in the loss function, which controls the training of the differential operator term, and we will take $\lambda \geq 1$ (see further discussion in Section 3), because when training the network, we want it to focus on the differential operator since this is more related to the accuracy of the approximation. Second, we do not include a term in the loss function corresponding to the boundary condition (16). The reason is that in this paper we solve the Cauchy problem (11)-(12) which does not have a boundary condition. As is typical for all solvers of the Cauchy problems, we solve the PDE problem in a sufficiently large computational space domain G , so that the domain of interest in pricing is smaller than G to avoid imposing boundary conditions.

The idea of solving PDE problems by DGM is that, by using stochastic gradient descent and back propagation from the deep learning algorithms (Goodfellow et al. 2016), one can efficiently find the set of neural network parameters $\boldsymbol{\theta}$ which minimise the loss function $L(f)$. Note that DGM solves PDE problems without building a mesh. We also remark that the deep learning approach allows us to break away from the “curse of dimensionality” and efficiently solve high-dimensional PDEs, including high-dimensional parametric PDEs as shown in this paper.

2.3.2 The DGM algorithm

To achieve the goal from the previous subsection, the minimisation of the loss function, in practice, we generate random sample points in $[0, T] \times G$ to calculate the loss function $L(f)$ (the forward propagation step), and then use stochastic gradient descent to minimise the loss function $L(f)$ (Goodfellow et al. 2016).

The DGM algorithm adapted for our setup begins by initialising its parameters θ with some θ_0 , followed by the loss optimisation loops. The n th loop is as follows:

1. For the differential operator term, generate random points (t_n, \mathbf{x}_n) from $[0, T] \times G$ according to the joint uniform distribution density ν_1 on $[0, T] \times G$; for the terminal condition term, generate the random points \mathbf{w}_n from G according to the uniform distribution density ν_2 on G .
2. Calculate the squared error $G(\theta_n, \mathbf{s}_n)$ at the randomly sampled points $\mathbf{s}_n = \{(t_n, \mathbf{x}_n), \mathbf{w}_n\}$:

$$G(\theta_n, \mathbf{s}_n) = \lambda \left(\frac{\partial}{\partial t} f(t_n, \mathbf{x}_n; \theta_n) + \mathcal{L}f(t_n, \mathbf{x}_n; \theta_n) \right)^2 + (f(T, \mathbf{w}_n; \theta_n) - u_T(\mathbf{w}_n))^2. \quad (20)$$

3. Perform the gradient descent calculation to update the parameters θ using ADAM (Kingma & Ba 2014), a well known adaptive learning rate optimisation algorithm, at the random point \mathbf{s}_n with :

$$\theta_{n+1} = \theta_n - \alpha_n \nabla_{\theta} G(\theta_n, \mathbf{s}_n), \quad (21)$$

where α_n is the learning rate of optimisation algorithm which needs to be decreasing with n .

4. Repeat until a convergence criterion is satisfied. The convergence criterion could be $G(\theta_n, \mathbf{s}_n)$ smaller than some predetermined threshold, or $\|\theta_{n+1} - \theta_n\|_2$ smaller than some predetermined threshold.

As has been pointed out by Sirignano & Spiliopoulos (2018), θ_n will converge to a critical point of the objective function $L(f(\cdot; \theta))$ as $n \rightarrow \infty$; that is

$$\lim_{n \rightarrow \infty} \|\nabla_{\theta} L(f(\cdot; \theta_n))\|_2 = 0. \quad (22)$$

However, it is likely that θ_n only converges to a local minimum rather than a global minimum since the deep neural network $f(t, \mathbf{x}; \theta)$ is non-convex. It is for this reason that the hyperparameter $\lambda \geq 1$ in Eq. (20) is needed to improve the approximation.

The algorithm can solve the PDE problem (11)-(12) with varying time, t , and spot price, x , with other input parameters being fixed. Its extension to solving parametric PDE problems is explained and illustrated in Sections 3-5.

2.3.3 The deep neural network

It is known (see, e.g., Sirignano & Spiliopoulos 2018) that the speed of a neural network is problem dependent and it is important to choose an appropriate, problem-specific neural network structure to achieve reasonable training speed for a problem under consideration. Thanks to the activity of the machine learning community in the recent years, we can gain access to numerous neural network structures for PDE applications. The DGM network, used in this paper, can be considered as a variant of the widely used Long Short-Term Memory networks (LSTMs) introduced by Hochreiter & Schmidhuber (1997). LSTMs are a special kind of recurrent neural networks which are useful for modelling sequential data such as time series prediction or speech recognition problems. It is shown by Sirignano & Spiliopoulos (2018) that a LSTM type of architecture works well for PDE problems with ‘‘sharp turns’’ in the initial or terminal conditions, which is exactly the situation we have here, since we have a step function in the terminal condition of the backward Kolmogorov equation that we approximate.

Let us introduce the DGM neural network architecture:

$$\begin{aligned} \mathbf{S}^1 &= \vartheta(\mathbf{W}^1 \mathbf{x} + \mathbf{b}) \\ \mathbf{Z}^{\ell} &= \vartheta(\mathbf{U}^{z, \ell} \mathbf{x} + \mathbf{W}^{z, \ell} \mathbf{S}^{\ell} + \mathbf{b}^{z, \ell}), \quad \ell = 1, \dots, L, \\ \mathbf{G}^{\ell} &= \vartheta(\mathbf{U}^{g, \ell} \mathbf{x} + \mathbf{W}^{g, \ell} \mathbf{S}^{\ell} + \mathbf{b}^{g, \ell}), \quad \ell = 1, \dots, L, \\ \mathbf{R}^{\ell} &= \vartheta(\mathbf{U}^{r, \ell} \mathbf{x} + \mathbf{W}^{r, \ell} \mathbf{S}^{\ell} + \mathbf{b}^{r, \ell}), \quad \ell = 1, \dots, L, \\ \mathbf{H}^{\ell} &= \vartheta(\mathbf{U}^{h, \ell} \mathbf{x} + \mathbf{W}^{h, \ell} (\mathbf{S}^{\ell} \odot \mathbf{R}^{\ell}) + \mathbf{b}^{h, \ell}), \quad \ell = 1, \dots, L, \\ \mathbf{S}^{\ell+1} &= (1 - \mathbf{G}^{\ell}) \odot \mathbf{H}^{\ell} + \mathbf{Z}^{\ell} \odot \mathbf{S}^{\ell}, \quad \ell = 1, \dots, L, \\ f(\mathbf{x}; \theta) &= \mathbf{W} \mathbf{S}^{L+1} + \mathbf{b}, \end{aligned}$$

where \mathbf{x} denotes the input layer, $\vartheta(\cdot)$ is the activation function, \odot denotes the element-wise multiplication, the number of hidden layers is $L + 1$, and \mathbf{U} , \mathbf{W} , \mathbf{b} are the parameters of the network. The input \mathbf{x} can be just (t, \mathbf{x}) from $[0, T] \times G$ for solving a PDE problem with fixed parameters as it is in the previous subsection or, in addition, can also include parameters of the PDE when we solve parametric PDE problems as in the following sections. We note that we use the same letter f in slightly different contexts but this should not lead to any confusion.

A neural network with this LSTM-like architecture is quite complex, consisting of a chain of hidden layers with each hidden layer containing sub-layers. Sirignano & Spiliopoulos (2018) suggest using the following hyperparameters (the set of parameters that controls the network architecture and the learning process): four hidden layers in the network ($L = 3$), 50 nodes per layer ($M = 50$), using hyperbolic tangent function as the activation function $\vartheta(\cdot)$, which guarantees that $f(\mathbf{x}; \boldsymbol{\theta})$ is smooth and, hence, is suitable for approximating the classical solution of the PDE. Xavier initialisation is used to initialise parameters and, as noted earlier, the ADAM optimisation algorithm is used to update the parameters. The learning rate α_n from Eq. (21) follows a decaying piecewise constant schedule:

$$\alpha_n = \begin{cases} 10^{-4} & n \leq 5,000 \\ 5 \times 10^{-5} & 5,000 < n \leq 10,000 \\ 10^{-5} & 10,000 < n \leq 20,000 \\ 5 \times 10^{-6} & 20,000 < n \leq 30,000 \\ 10^{-6} & 30,000 < n \leq 40,000 \\ 5 \times 10^{-7} & 40,000 < n \leq 50,000 \\ 10^{-7} & 50,000 < n \leq 100,000 \\ 5 \times 10^{-8} & 100,000 < n \leq 200,000 \\ 10^{-8} & n > 200,000. \end{cases}$$

We implement this algorithm in TensorFlow, which is the open-source software library developed by Google and designed specifically for deep learning. TensorFlow has a built-in function for parameter initialisation and optimisation algorithms. This allows great simplification of our neural network development process.

For demonstrations in this paper, we use 5,000 sample points per epoch. An epoch means passing the entire 5,000 randomly generated dataset backward and forward through the neural network. An epoch trains on 5,000 random sample points with 5 mini-batches and 1,000 sample points per mini-batch. Training on mini-batches rather than on the entire dataset improves the efficiency of the stochastic gradient descent of deep learning training. Problems of different complexity require different number of epochs to reach the required accuracy. The number of epochs here is related to the total number of random points we need to generate. We performed the deep learning training via the Google Colab Pro server, where we used a single NVIDIA Tesla P100 GPU.

3 Geometrical Brownian motion

First, we illustrate our implementation using geometrical Brownian motion as in the derivation of the Black-Scholes-Merton formula (Black & Scholes 1973; Merton 1973). Under the forward measure of the log asset price space, the backward Kolmogorov equation for the CDF $C(t, x) = C(t, x; T, y)$ is

$$\frac{\partial C}{\partial t} - \frac{\sigma^2}{2} \frac{\partial C}{\partial x} + \frac{\sigma^2}{2} \frac{\partial^2 C}{\partial x^2} = 0, \quad t \in [0, T), \quad x \in \mathbb{R}, \quad (23)$$

with terminal condition

$$C(T, x) = \mathbb{1}(x \leq y) = \begin{cases} 1, & x \leq y, \\ 0, & x > y. \end{cases} \quad (24)$$

To find the TPDF from the cumulative distribution, we must first solve the backward Kolmogorov equation in a parametric manner for a range of $y \in [y_{\min}, y_{\max}]$, given a minimum value of the range y_{\min} and a maximum value y_{\max} , so that after taking the derivative of $C(t, x; T, y)$ with respect to y , we obtain the TPDF $p(t, x; T, y)$. Also, from the underlying asset process, we have that the CDF is a function of the volatility, σ . Thus, the problem needs to be solved in the (t, x, y, σ) -domain $Q \subset \mathbb{R}^4$, which contains not only the independent variables $(t, x) \in [0, T] \times G \subset \mathbb{R}^2$ with respect to which the PDE is formulated, but also the parameters $(y, \sigma) \in \mathbb{R}^2$. Using the artificial neural network $f(\mathbf{x}; \boldsymbol{\theta}) = f(t, x, y, \sigma; \boldsymbol{\theta})$ described in the previous section, we can find a solution to the parametric problem for the backward Kolmogorov equation.

The optimisation process starts with initialising the network parameters $\boldsymbol{\theta}$. Then, for each epoch, we uniformly sample points from Q before feeding them to the DGM network and then using gradient descent optimisation algorithm to minimise the loss function. The process is repeated until the required accuracy is reached. The loss function in this

example is defined as

$$L_1(f) = \left\| \left(\frac{\partial}{\partial t} - \frac{1}{2}\sigma^2 \frac{\partial}{\partial x} + \frac{1}{2}\sigma^2 \frac{\partial^2}{\partial x^2} \right) f(t, x, y, \sigma; \boldsymbol{\theta}) \right\|_{[0, T] \times G, \nu_1}^2, \quad (25)$$

$$L_2(f) = \|f(T, x, y, \sigma; \boldsymbol{\theta}) - \mathbb{1}(x \leq y)\|_{G, \nu_2}^2, \quad (26)$$

$$L(f) = \lambda L_1(f) + L_2(f). \quad (27)$$

The first and second partial derivatives terms $\partial f/\partial t$, $\partial f/\partial x$, and $\partial^2 f/\partial x^2$ can be either computed directly using the gradient function in TensorFlow (or similar derivatives calculation functions in other deep learning libraries) or approximated via numerical differentiation with finite differences.

The domain Q we use to train the network is $x, y \in [-2.3, 2.3]$, $\sigma \in [0, 0.6]$, $t \in [0, 1.2]$. This means that the time horizon for the network is $T = 1.2$. We also note that $T - t$ is the time to maturity, which in future we will often denote as T again, but this should not cause any confusion. Note that although we fix the log-spot price $x_0 = 0$, we still need to train the network in x as the PDE is written in x . We train 100,000 epochs. For each epoch, we use 5000 random points with 5 mini-batches. Thus, in total, we use 500 million random space time points to train this network. We train for different loss control parameters $\lambda = 1, 10, 100$. We compare the obtained approximation \tilde{p} of the density function p , which is Gaussian and has the closed form in this case:

$$p(0, x; T, y) = \frac{1}{\sigma\sqrt{2\pi T}} \exp\left[-\frac{(x - y + 0.5\sigma^2 T)^2}{2\sigma^2 T}\right]. \quad (28)$$

Training results are shown in Figure 1. Compared with $\lambda = 1$, when $\lambda = 10$, L_1 loss is one order of magnitude more accurate while L_2 loss is at the same order of magnitude; when $\lambda = 100$, L_1 loss is two orders of magnitude more accurate while L_2 loss is considerably less accurate. We make a recommendation for a choice of λ later in this section after we analyse approximations of the quantities of interest (TPDF and an option price).

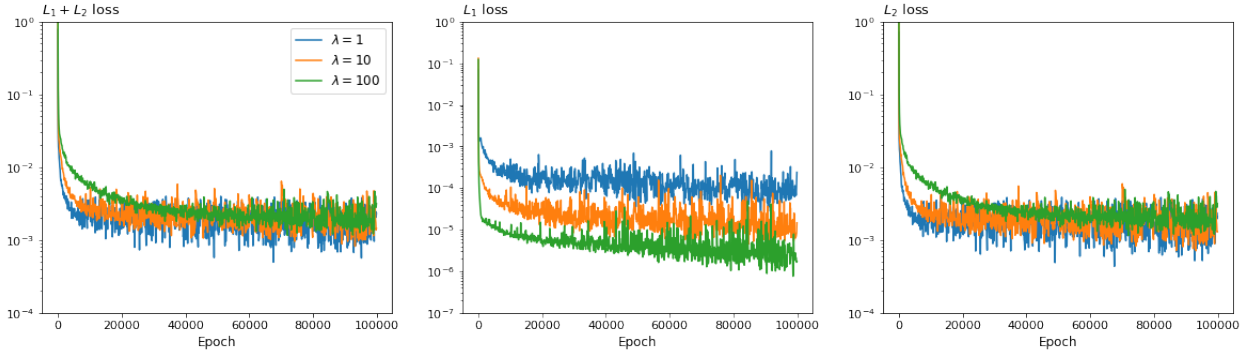


Figure 1: Plots of model losses for $\lambda = 1, 10, 100$.

Table 1: Root mean squared errors (RMSE) for $\lambda = 1, 10, 100$ compared with closed form density solution. The parameters: y has 10,000 evenly spaced samples, calculated over interval $[-2, 2]$. $x = 0$, $\sigma = 0.25$. Time to maturity $T = 0.1, 0.25, 0.5, 0.75, 1.0$.

T	$\lambda = 1$	10	100
0.1	0.032	0.019	0.059
0.25	0.016	0.008	0.025
0.5	0.011	0.006	0.011
0.75	0.008	0.005	0.007
1.0	0.006	0.005	0.006

Once the cumulative distribution function $C(t, x; T, y) = C(t, x; T, y, \sigma)$ has been approximated (via the network training) by $f(\mathbf{x}; \boldsymbol{\theta}) = f(t, x, y, \sigma; \boldsymbol{\theta})$, we use numerical differentiation to approximate the transition probability $p(t, x; T, y) = p(0, x; T - t, y, \sigma)$ by $\tilde{p}(0, x; T - t, y) = \tilde{p}(0, x; T - t, y; \boldsymbol{\theta})$:

$$\tilde{p}(0, x; T - t, y) = \frac{f(t, x, y + \Delta, \sigma; \boldsymbol{\theta}) - f(t, x, y - \Delta, \sigma; \boldsymbol{\theta})}{2\Delta} \quad (29)$$

for some $\Delta > 0$. In our experiments we chose $\Delta = 0.005$. The choice of Δ should be neither too small nor too large: if it is too small, that could introduce oscillation and the density would not be smooth; if it is too large, the approximation accuracy around the peak area of the density is insufficient. We find that a good choice of Δ is in the range of $[0.001, 0.01]$.

Table 1 shows the root mean squared errors (RMSEs) for $\lambda = 1, 10, 100$ across different maturities. We see that deep learning approximation does indeed generate very accurate results compared to closed form solutions. The results show that the $\lambda = 10$ case performs best. Differential operator L_1 loss is more relevant to the overall accuracy values of the solution while the terminal condition L_2 loss is related to the areas around the “sharp turns” of the solution. The case with $\lambda = 10$ strikes the right balance between the two losses. This demonstrates that the loss control parameter λ is useful when performing training. Figure 2 shows the approximated transition density compared with the exact closed form solution.

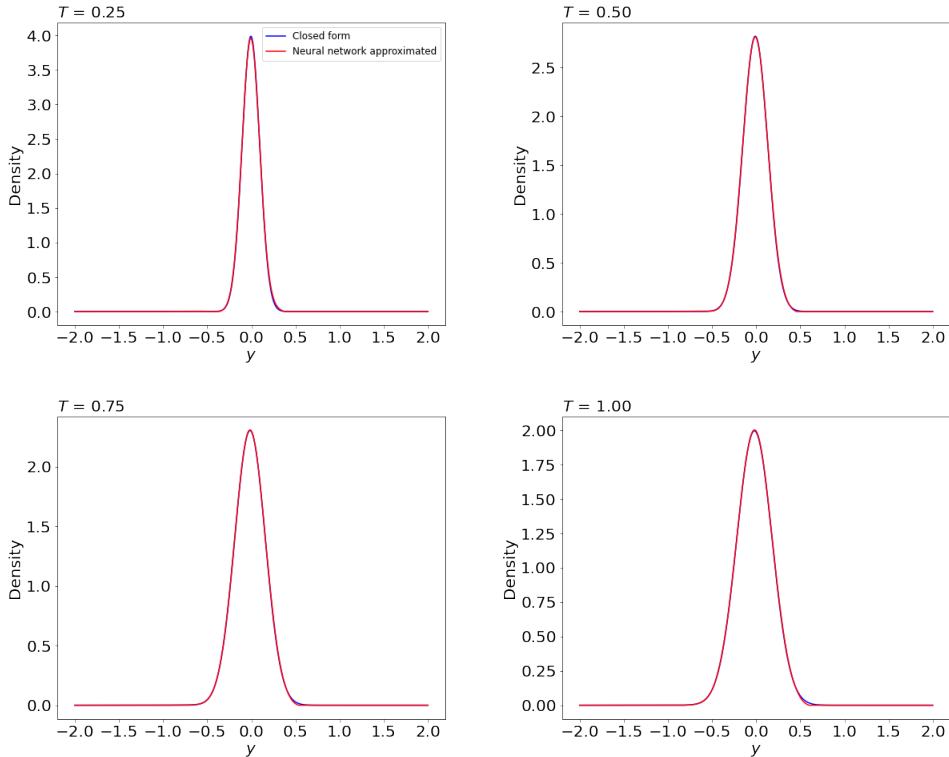
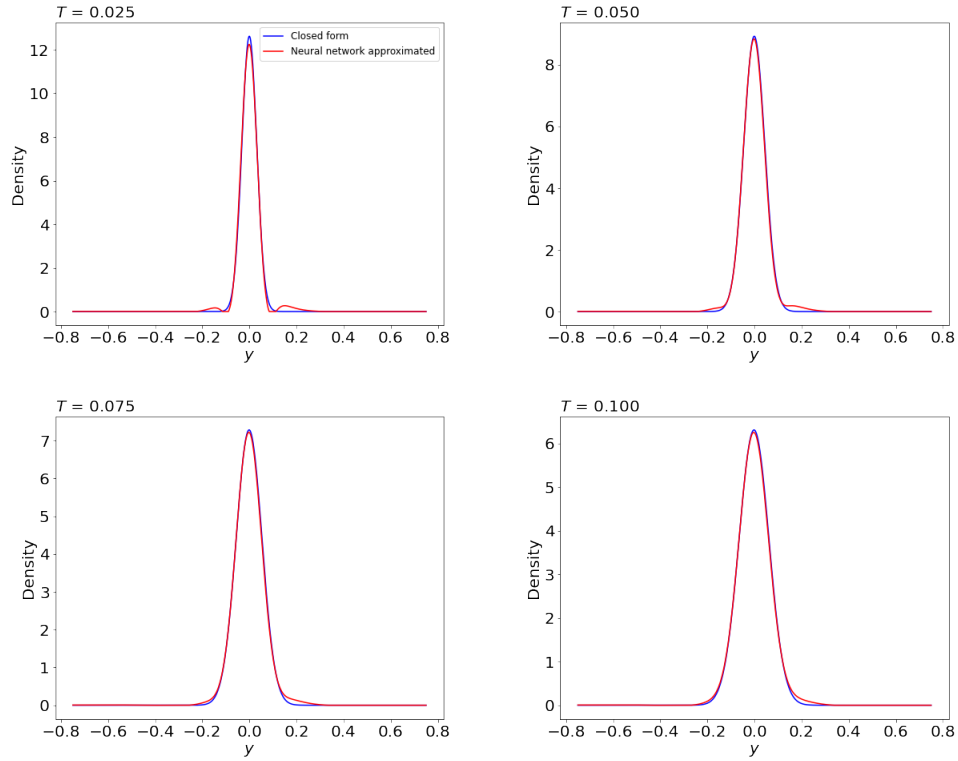
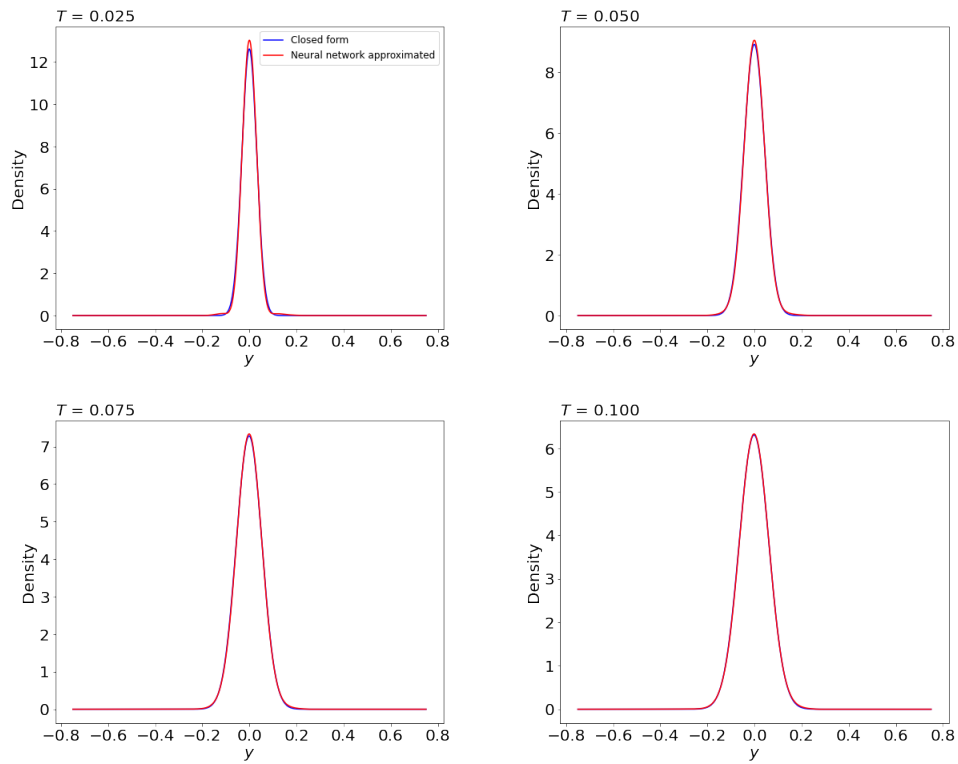


Figure 2: Gaussian TPDF, closed form vs. neural network approximated. $x = 0$, $\sigma = 0.25$, the time to maturity $T = 0.25, 0.5, 0.75, 1.0$. The domain we use to train the network is $x, y \in [-2.3, 2.3]$, $\sigma \in [0, 0.6]$, $t \in [0, 1.2]$.

From Table 1, we notice that when T is decreased, the approximation accuracy decreases. This can also be seen in Figure 3a. This result is not surprising: when T gets smaller, the TPDF concentrates around the initial state (0 in this example) and derivatives of the CDF C with respect to y tend to infinity when T goes to 0 (see Eqs. (13) and (24)) affecting accuracy of numerical differentiation. If the training range is too broad ($[-2.3, 2.3]$ in this example), the narrow range around the zero initial state may not acquire sufficient data points, resulting in less than optimal approximations compared with larger T . If we did not train specifically for T being close to 0, the approximation accuracy for this region could be low. We have a straightforward and efficient solution to this problem, via transfer learning. This is a common strategy to train a new model for a related problem using existing knowledge. Here, we transfer the model we have for one domain to another. If the transition probability density function with smaller T is what we require, we can perform transfer learning and use a pre-trained model to train for the smaller T . Transfer learning is much more efficient than training from scratch. For instance, here we use the model we have trained on the domain as defined above and then change the domain Q to the new domain $x, y \in [-0.75, 0.75]$, $\sigma \in [0, 0.6]$, $t \in [0, 0.12]$. With another 10,000 epochs of training, we can have a well-fitting model that is dedicated for smaller T . This is illustrated in Figure 3b. Similarly, when we need a result that is out of the training domain range, we can use the transfer learning idea to obtain the required result efficiently.



(a) TPDF results based on the model as in Figure 2, compared with closed form solutions.



(b) TPDF results after transfer learning after 10,000 epochs, compared with closed form solutions. Training domain for the transfer learning is $x, y \in [-0.75, 0.75]$, $\sigma \in [0, 0.6]$, $t \in [0, 0.12]$.

Figure 3: Gaussian TPDF, closed form vs. neural network approximated for small time to maturity. $x = 0$, $\sigma = 0.25$, the time to maturity $T = 0.025, 0.05, 0.075, 0.1$.

Next, we test the results with QUAD applications. Once offline training of the artificial neural network has been completed, it can be used online for pricing any options for this underlying model (within the range of volatility σ and maturity T for which the network was trained). This is unlike conventional numerical methods, which have to be run online for each set of the parameters' values separately that is considerably slower than taking the required values from a trained neural network.

We train our network on Google's Colab Pro server with a NVIDIA Tesla P100 GPU and use the network along with the QUAD method on a standard desktop with an Intel i7-9700k CPU and NVIDIA RTX 2070 GPU. We price European options with the approximated density and compare with results obtained using the true density. Table 2 shows that the pricing performance using QUAD with the neural network approximated density is excellent. This brings us to an important feature of replacing previous calculation engines for TPDF with one developed through deep learning: accessing a trained neural network to retrieve the density takes very little time, meaning that calculating a single option using neural network density with QUAD is as fast as using the closed form density with QUAD. This preserves the immense speed advantage of not just the original QUAD shown in Andricopoulos et al. (2003) but for more complex models of the underlying which had previously slowed the QUAD calculations; e.g. in Chen et al. (2014). We illustrate this in later sections. More exotic options could also be priced using QUAD with an artificial neural network approximated density but we need not demonstrate this here, since these have been shown for geometrical Brownian motion in the earlier QUAD papers.

Table 2: RMSE of QUAD pricing using neural network approximated density, benchmarked against closed form density pricing. Initial price is $S_0 = 1$, strike price K , volatility σ , and time to maturity T are randomly sampled as $K \in [0.8, 1.2]$, $\sigma \in [0.1, 0.4]$, $T \in [0.1, 1.1]$. The number of random cases is 10,000 each for both call and put prices.

	European call	European put
RMSE	2.199×10^{-3}	1.182×10^{-3}

TPDFs for other one-dimensional processes such as constant elasticity of variance (CEV) process, Vasicek /Ornstein–Uhlenbeck (OU) process can be approximated in similar fashion via deep learning. This approach can also be applied to the case of Merton's jump diffusion process. We note that the backward Kolmogorov equations for jump processes take the form of partial integro-differential equations (Applebaum 2009), which are more complex than the backward Kolmogorov equation for the diffusion-type models we deal with here but, as it has been pointed out by Sirignano & Spiliopoulos (2018), these equations can be solved with a similar algorithm.

4 The Heston model

Next, we illustrate how to use deep learning to find the joint probability density in a more complicated two-dimensional case, Heston's (1993) stochastic volatility model.

Under the forward measure, the Heston model assumes log stock price, X , and variance, V , of the stock price to follow the system of SDEs

$$dX = -\frac{V}{2}dt + \sqrt{V}dW_t^X, \quad (30)$$

$$dV = \kappa(\theta - V)dt + \xi\sqrt{V}dW^V, \quad (31)$$

$$dW^X dW^V = \rho dt, \quad (32)$$

where W^X, W^V are Wiener processes with correlation ρ , θ represents the long term variance, κ is the rate at which V reverts to θ , ξ is the volatility of the volatility (vol of vol). We require that $2\kappa\theta \geq \xi^2$ to ensure that the variance process is strictly positive at any finite time.

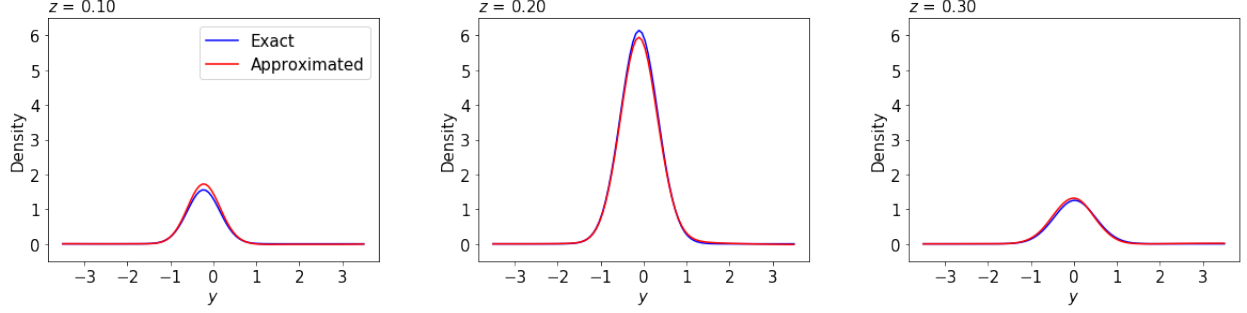
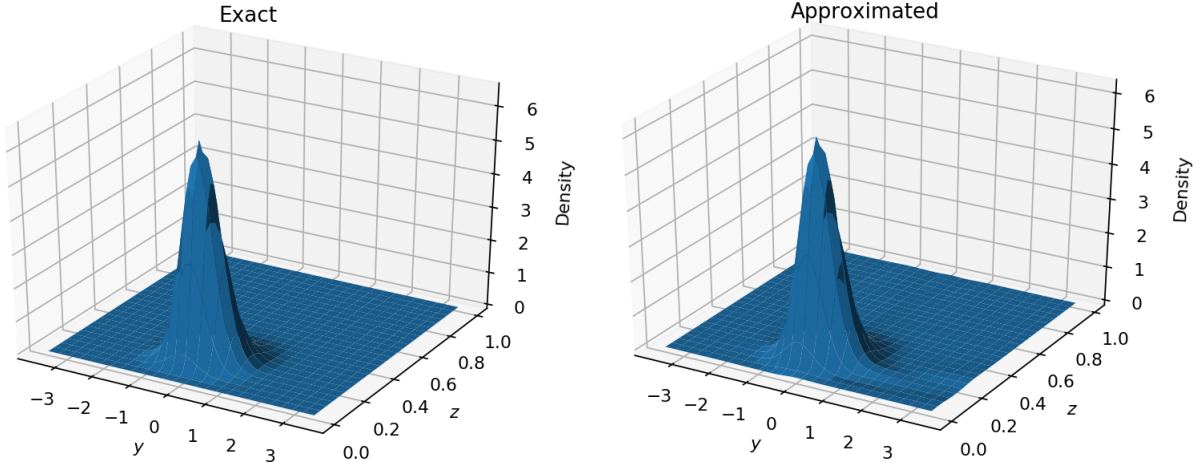
The backward Kolmogorov equation for the joint CDF $C(t, x, v) = C(t, x, v; T, y, z)$ is

$$\frac{\partial C}{\partial t} - \frac{v}{2} \frac{\partial C}{\partial x} + (\kappa(\theta - v)) \frac{\partial C}{\partial v} + \frac{1}{2}v \frac{\partial^2 C}{\partial x^2} + \frac{1}{2}\xi^2 v \frac{\partial^2 C}{\partial v^2} + \rho\xi v \frac{\partial^2 C}{\partial x \partial v} = 0, t \in [0, T), x \in \mathbb{R}, v > 0, \quad (33)$$

with terminal condition

$$C(T, x, v) = \mathbb{1}(x \leq y, v \leq z) = \begin{cases} 1, & x \leq y \text{ and } v \leq z, \\ 0, & \text{otherwise.} \end{cases} \quad (34)$$

Note that this PDE problem is of the form (14)-(15).


 (a) 2D graphs by changing terminal variance $z = 0.1, 0.2, 0.3$.


(b) 3D graphs

Figure 4: Transition probability density graphs comparison in the case of the Heston model. The parameters are $x = 0$, $v = 0.2$, $\kappa = 1.0$, $\theta = 0.2$, $\xi = 0.2$, $\rho = 0.2$. Time to maturity $T = 1.0$. “Exact” means the exact Heston density obtained by the semi-closed form from Lewis (2016), “Approximated” means the approximation due to the trained neural network.

We build an artificial neural network, f , to approximate the CDF, C . For the Heston model, the neural network f is trained in the $(t, x, y, v, z, \kappa, \theta, \xi, \rho)$ -domain $Q \subset \mathbb{R}^9$, which is high-dimensional. Traditional methods aimed at solving PDEs under fixed parameters are uncompetitive in this challenging parametric PDE setting in comparison with the deep-learning algorithm. We note that the high-dimensionality here is of the parametric space. We recall that we need to solve high-dimensional parametric PDEs to find TPDFs for a range of values in the time-state and parametric spaces in order to effectively use the TPDFs for financial engineering tasks such as pricing options. The problem (14)-(15) is higher dimensional and more complicated than the geometric Brownian motion case in Section 3. Therefore, it can be expected that the numbers of epochs and sample points will be larger. We follow the same training process as in the previous section with evident adjustments.

Similar to the geometric Brownian motion case, we calculate the joint transition probability for the spot log-price $x_0 = 0$. Here, with Heston’s model, we choose Q as $x, y \in [-3.5, 3.5]$, $v, z \in [0, 1]$, $\kappa \in [0.8, 1.2]$, $\theta \in [0.1, 0.3]$, $\xi \in [0, 0.3]$, $t \in [0, 1.2]$. To attain the required accuracy, we find that $\lambda = 100$ is suitable, and we train 400,000 epochs and 5,000 points per epoch, which is equivalent to using 2 billion sample points to train this network. We select the epoch training that has the lowest loss.

We compare the approximate joint TPDF with the semi-closed form of the TPDF from Lewis (2016). We find that the approximate TPDF is close to the true TPDF, as shown in Figure 4. The RMSEs of the artificial neural network approximated density are shown in Table 3. The reason why RMSE for smaller T is larger is that the density value range for small T is also wider.

We compare the pricing performance incorporated into QUAD. As can be seen in Table 4, the pricing results using the artificial neural network approximated joint TPDF produce sufficiently accurate results when compared with the

Table 3:

RMSEs in the case of the Heston model, compared against the exact TPDF. Parameters are $x = 0, v = 0.2, \kappa = 1.0, \theta = 0.2, \xi = 0.2, \rho = 0.2$. Time to maturity $T = 0.25, 0.5, 0.75, 1.0$.

T	RMSE
0.25	0.104
0.5	0.049
0.75	0.036
1.0	0.030

Table 4:

Heston model. European call pricing results with QUAD using the neural network approximated density and semi-closed form density. QUAD is using 51 mesh points per direction, so there are total 2601 points. Initial price $S_0 = 1.0$. K is the strike of the option. Pricing times are in parentheses.

$(K, v, T, \kappa, \theta, \xi, \rho)$	QUAD with semi-closed form	QUAD with NN approximated
(1.0, 0.2, 1.0, 1.0, 0.2, 0.2, 0.2)	0.179(13.18 seconds)	0.180 (0.53 seconds)
(1.05, 0.2, 0.75, 1.0, 0.2, 0.2, 0.2)	0.138(13.53 seconds)	0.137 (0.45 seconds)
(0.9, 0.2, 0.5, 1.0, 0.2, 0.2, 0.2)	0.175 (12.5 seconds)	0.179 (0.46 seconds)
(1.0, 0.2, 0.25, 1.0, 0.2, 0.2, 0.2)	0.089 (11.75 seconds)	0.093 (0.51 seconds)
(0.95, 0.1, 0.7, 1.0, 0.09, 0.25, 0.1)	0.127 (12.73 seconds)	0.130 (0.46 seconds)
(1.1, 0.15, 1.0, 1.0, 0.09, 0.2, 0.3)	0.105 (12.17 seconds)	0.104 (0.51 seconds)
(1.03, 0.3, 0.2, 1.0, 0.2, 0.15, 0.2)	0.083 (11.03 seconds)	0.088 (0.53 seconds)
(0.88, 0.1, 0.8, 1.0, 0.12, 0.25, 0.25)	0.177 (12.71 seconds)	0.176 (0.56 seconds)

semi-closed form solutions. At this point, we highlight a considerable advantage of the neural network over semi-closed solutions. Based on QUAD calculation with 51 mesh points per direction, QUAD with approximated density is 20 times faster than using semi-closed form solutions. If we increase the number of mesh points per direction to 101, that is 10201 points in the QUAD mesh, the speed advantage is 40 times. In practice, QUAD with 51 mesh points per direction can produce very accurate results. The artificial neural network approximated density is very fast to evaluate, close to the speed of using closed form solutions, and it is a perfect match with QUAD.

Stochastic volatility processes, such as the SABR process, 3/2 process, or stochastic volatility jump diffusion processes can, likewise, be treated in this way.

5 Heston model with time-dependent parameters

We next demonstrate that a version of the Heston model with time-dependent parameters can also be handled. We note that a closed-form density for this model is not available. The model considered in this section was proposed by Mikhailov & Nögel (2003) and also Benhamou, Gobet & Miri (2010), where it was shown that this model can reproduce the volatility smile better than the plain Heston model. Conventional density approximation methods may not be able to handle the complicated structure of the time-dependent processes, but the deep learning method we present here is very flexible and it is able to approximate the density through training.

The set up of the Heston model with time-dependent parameters is similar to that for the plain Heston model (30). The stochastic processes for log stock price X and variance V satisfy the system of SDEs under the forward measure:

$$dX = -\frac{V}{2}dt + \sqrt{V}dW_t^X, \tag{35}$$

$$dV = \kappa(\theta_t - V)dt + \xi_t\sqrt{V}dW^V, \tag{36}$$

$$dW^X dW^V = \rho_t dt, \tag{37}$$

where the long term variance θ_t , volatility of volatility ξ_t , and the correlation coefficient ρ_t are time-dependent deterministic functions. We require that $2\kappa\theta_t \geq \xi_t^2$ to ensure that the variance process is strictly positive at any finite time.

Table 5:

Put option price comparison for the time-dependent Heston model for various maturity times t and strike prices K . Computing time is in parentheses. “NN” refers to the put prices using QUAD with the neural network approximated density, while “Ave” refers to approximating the plain Heston model using average parameters as in Benhamou et al. (2010) and then using QUAD to price put options. We use the equivalent average parameters suggested in that paper: for time to maturity $T = 0.25$, $(\bar{v}, \bar{\theta}_t, \bar{\xi}_t, \bar{\rho}_t) = (0.04, 0.04, 0.3, -0.2)$; for $T = 0.5$, $(\bar{v}, \bar{\theta}_t, \bar{\xi}_t, \bar{\rho}_t) = (0.0397, 0.0404, 0.3012, -0.1993)$; for $T = 1.0$, $(\bar{v}, \bar{\theta}_t, \bar{\xi}_t, \bar{\rho}_t) = (0.0328, 0.0438, 0.3089, -0.1972)$.

$T \setminus K$		0.8	0.9	1.0	1.1	1.2
0.25	NN	0.002 (0.35s)	0.009 (0.29s)	0.041 (0.32s)	0.110 (0.40s)	0.201 (0.42s)
	Ave	0.001 (12.07s)	0.008 (11.15s)	0.039 (10.54s)	0.109 (10.39s)	0.201 (10.25s)
0.5	NN	0.005 (0.26s)	0.020 (0.34s)	0.057 (0.32s)	0.121 (0.35s)	0.205 (0.34s)
	Ave	0.004 (13.29s)	0.018 (12.58s)	0.055 (12.42s)	0.121 (12.06s)	0.206 (11.84s)
1.0	NN	0.013 (0.34s)	0.036 (0.40s)	0.078 (0.32s)	0.140 (0.35s)	0.218 (0.32s)
	Ave	0.013 (13.14s)	0.036 (13.09s)	0.078 (12.93s)	0.141 (12.75s)	0.219 (12.54s)

Similar to the plain Heston model Eqs. (33)-(34), the backward Kolmogorov equation for joint CDF $C(t, x, v) = C(t, x, v; T, y, z)$ is

$$\frac{\partial C}{\partial t} - \frac{1}{2}v \frac{\partial C}{\partial x} + (\kappa(\theta_t - v)) \frac{\partial C}{\partial v} + \frac{1}{2}v \frac{\partial^2 C}{\partial x^2} + \frac{1}{2}\xi_t^2 v \frac{\partial^2 C}{\partial v^2} + \rho_t \xi_t v \frac{\partial^2 C}{\partial x \partial v} = 0, \quad (38)$$

with terminal condition

$$C(T, x, v) = \mathbb{1}(x \leq y, v \leq z) = \begin{cases} 1, & x \leq y \text{ and } v \leq z, \\ 0, & \text{otherwise.} \end{cases} \quad (39)$$

To proceed further, we need to parameterise the time-dependent functions for θ_t , ξ_t and ρ_t first, before training. Here, we follow the set up of the piecewise-constant functions as in Benhamou et al. (2010). We train the approximated density for $t \in [0, 1.2]$. The initial variance is set to $v = 0.04$, mean reversion parameter $\kappa = 3$, the piecewise constant functions for the time dependent parameters in each given time interval are $\theta_t = 0.04 + i \times 0.0005$, $\xi_t = 0.3 + i \times 0.005$, $\rho_t = -0.2 + i \times 0.0035$, where $i = 0$ is for $t \in [0, 0.25]$, $i = 1$ is for $t \in (0.25, 0.5]$, $i = 2$ is for $t \in (0.5, 1.0]$, and $i = 3$ is for $t \in (1.0, 1.2]$. For the time-dependent Heston model, the neural network f is trained in the (t, x, y, v, z) -domain $Q \subset \mathbb{R}^5$. We choose the domain Q so that $x, y \in [-2.3, 2.3]$, $v, z \in [0, 0.4]$, $t \in [0, 1.2]$. To attain the required accuracy, we find that $\lambda = 100$ is suitable, and we train 400,000 epochs and 5,000 points per epoch, which is equivalent to using 2 billion sample points to train this network. We select the epoch training that has the lowest loss.

Since we have no closed form joint TPDF for the time-dependent Heston model, in order to test the effectiveness of the deep learning approximation, we compare the option pricing results. We first calculate put option prices directly using the artificial neural network approximated density with QUAD. Then we compare the results calculated by one of the approximation methods suggested in Benhamou et al. (2010) – through averaging Heston’s model parameters. Specifically, we calculate these benchmark options prices using QUAD under the averaging model. Table 5 compares the pricing results using artificial neural network approximated results against the benchmark. The pricing results are close to those using the benchmark, showing that the artificial neural network approximated time-dependent Heston density is indeed sufficiently accurate.

6 Conclusion

This paper is the first in the literature to use a deep learning approach in approximating transition probability density for any model of the underlying. Deep learning not only provides the required approximations but also its “single solve” capability across all parameters means that effort is expended only once in a single pre-computation, delivering a parametric PDE solver that does not require recalibration.

Instead of aiming at directly solving the forward Kolmogorov (Fokker-Planck) equation for transition density which would require handling the initial condition (a “nasty” Dirac delta function) we use an ingenious way of first solving the backward Kolmogorov equation for cumulative probability function which involves the terminal condition, a more “tamable” step function, before calculating transition density by differentiating the cumulative probability. We train an artificial neural network by optimising a purposefully constructed cost function, thereby solving the governing partial differential equation for the cumulative distribution function of any given underlying price process. For this, we can use as much simulated data as needed in order to train offline a deep neural network. Once the network is trained, we have an ultra-fast transition density generator, tailored to the underlying model and portable to other calculation setups

and computers. We demonstrate first for the simple Black-Scholes-Merton setup, noting that valuations with other one-dimensional processes as underlyings can likewise be solved, as can Merton's jump diffusion process. Next we use Heston's model (1993) as an example of stochastic volatility models which can be handled. To confirm to versatility of the method, we conclude by showing how to solve options valuations with a time-dependent version of the Heston model as the underlying, for which there is no available closed form joint TPDF.

The applications of learning the transition density using deep neural networks go beyond those illustrated, such as likelihood inference and default probability calculation in credit risk management. Options are ubiquitous in finance, from the large range of directly available options on exchanges and over-the-counter, to credit risk and Real Options. During the five decades since the founding framework of Black, Scholes and Merton, practitioners and academics have developed ways of dealing with option features (such as early exercise) in combination with models of the underlying (such as Heston's) but often either the models are too simple or the solutions too hard. Although parallel computing, using GPUs, speeds up conventional approaches (indeed, investment banks may use hundreds or even thousands of these to accelerate parallel calculations) nevertheless, massive calculations still need to be repeated in frequent recalibrations. The deep learning approach we describe avoids this. The promise of targeted deep learning, as begun in this paper, is for development of suites of fast, flexible programs to tackle the full range of models and applications.

References

- Aït-Sahalia, Y. (2002), 'Maximum likelihood estimation of discretely sampled diffusions: a closed-form approximation approach', *Econometrica* **70**, 223–262.
- Aït-Sahalia, Y. (2008), 'Closed-form likelihood expansions for multivariate diffusions', *Annals of Statistics* **36**, 906–937.
- Al-Aradi, A., Correia, A., Naiff, D., Jardim, G. & Saporito, Y. (2018), 'Solving nonlinear and high-dimensional partial differential equations via deep learning', *arXiv preprint arXiv:1811.08782*.
- Andricopoulos, A. D., Widdicks, M., Duck, P. W. & Newton, D. P. (2003), 'Universal option valuation using quadrature methods', *Journal of Financial Economics* **67**, 447–471. (See also Corrigendum, *Journal of Financial Economics* **73**, 603 (2004)).
- Andricopoulos, A. D., Widdicks, M., Newton, D. P. & Duck, P. W. (2007), 'Extending quadrature methods to value multi-asset and complex path dependent options', *Journal of Financial Economics* **83**, 471–499.
- Antoulas, A. C., Ionutiu, R., Martins, N., ter Maten, E. J. W., Mohaghegh, K., Pulch, R., Rommes, J., Saadvandi, M. & Striebel, M. (2015), Model order reduction: Methods, concepts and properties, in M. Günther, ed., 'Coupled Multiscale Simulation and Optimization in Nanoelectronics', Springer, Berlin, pp. 159–265.
- Applebaum, D. (2009), *Lévy processes and stochastic calculus*, Cambridge University Press, Cambridge.
- Benhamou, E., Gobet, E. & Miri, M. (2010), 'Time dependent Heston model', *SIAM Journal on Financial Mathematics* **1**, 289–325.
- Black, F. & Scholes, M. (1973), 'The pricing of options and corporate liabilities', *Journal of Political Economy* **81**, 637–654.
- Chen, D., Härkönen, H. J. & Newton, D. P. (2014), 'Advancing the universality of quadrature methods to any underlying process for option pricing', *Journal of Financial Economics* **114**, 600–612.
- Cosma, A., Galluccio, S., Pederzoli, P. & Scaillet, O. (2020), 'Early exercise decision in American options with dividends, stochastic volatility, and jumps', *Journal of Financial and Quantitative Analysis* **55**, 331–356.
- Cox, J. C. (1996), 'The constant elasticity of variance option pricing model', *Journal of Portfolio Management* **23**, 15–17.
- Cox, J. C., Ingersoll Jr, J. E. & Ross, S. A. (1985), 'An intertemporal general equilibrium model of asset prices', *Econometrica* **53**, 363–384.
- Dissanayake, M. & Phan-Thien, N. (1994), 'Neural-network-based approximations for solving partial differential equations', *Communications in Numerical Methods in Engineering* **10**, 195–201.
- Figlewski, S. (2009), 'Estimating the implied risk-neutral density for the us market portfolio, volatility and time series econometrics: essays in honor of Robert F. Engle'.
- Figlewski, S. (2018), 'Risk-neutral densities: A review', *Annual Review of Financial Economics* **10**, 329–359.
- Filipović, D., Mayerhofer, E. & Schneider, P. (2013), 'Density approximations for multivariate affine jump-diffusion processes', *Journal of Econometrics* **176**, 93–111.
- Floc'h, L. & Kennedy, G. J. (2014), 'Finite difference techniques for arbitrage free SABR', Available at SSRN 2402001

- Freidlin, M. I. (1985), *Functional integration and partial differential equations*, Princeton Univ. Press, Princeton.
- Gardiner, C. W. (2004), *Handbook of stochastic methods for physics, chemistry and the natural sciences*, Springer, Berlin.
- Geist, M., Petersen, P., Raslan, M., Schneider, R. & Kutyniok, G. (2020), ‘Numerical solution of the parametric diffusion equation by deep neural networks’, *arXiv preprint arXiv:2004.12131* .
- Gichman, I. I. & Skorochod, A. V. (1972), *Stochastic differential equations*, Springer, Berlin.
- Goodfellow, I., Bengio, Y. & Courville, A. (2016), *Deep Learning*, MIT press.
- Hagan, P. S., Kumar, D., Lesniewski, A. S. & Woodward, D. E. (2002), ‘Managing smile risk’, *The Best of Wilmott* **1**, 249–296.
- Hagan, P. S., Kumar, D., Lesniewski, A. & Woodward, D. (2014), ‘Arbitrage-free SABR’, *Wilmott* **2014**, 60–75.
- Henry-Labordère, P. (2008), *Analysis, geometry, and modeling in finance: Advanced methods in option pricing*, CRC Press.
- Heston, S. L. (1993), ‘A closed-form solution for options with stochastic volatility with applications to bond and currency options’, *Review of Financial Studies* **6**, 327–343.
- Heston, S. L. (1997), ‘A simple new formula for options with stochastic volatility’, *Available at SSRN 86074* .
- Hinton, G. E., Osindero, S. & Teh, Y.-W. (2006), ‘A fast learning algorithm for deep belief nets’, *Neural computation* **18**, 1527–1554.
- Hochreiter, S. & Schmidhuber, J. (1997), ‘Long short-term memory’, *Neural computation* **9**, 1735–1780.
- Hutchinson, J. M., Lo, A. W. & Poggio, T. (1994), ‘A nonparametric approach to pricing and hedging derivative securities via learning networks’, *Journal of Finance* **49**, 851–889.
- Khoo, Y., Lu, J. & Ying, L. (2017), ‘Solving parametric pde problems with artificial neural networks’, *arXiv:1707.03351* .
- Kingma, D. P. & Ba, J. (2014), ‘Adam: A method for stochastic optimization’, *arXiv preprint arXiv:1412.6980* .
- Kutyniok, G., Petersen, P., Raslan, M. & Schneider, R. (2019), ‘A theoretical analysis of deep neural networks and parametric PDEs’, *arXiv preprint arXiv:1904.00377* .
- Ladyzhenskaya, O., Solonnikov, V. & Ural’tseva, N. N. (1968), *Linear and quasi-linear equations of parabolic type*, Vol. 23 of *Trans. Math. Monog.*, Amer. Math. Soc., Providence, RI.
- Lagaris, I. E., Likas, A. C. & Papageorgiou, D. G. (2000), ‘Neural-network methods for boundary value problems with irregular boundaries’, *IEEE Transactions on Neural Networks* **11**, 1041–1049.
- Lagaris, I. E., Likas, A. & Fotiadis, D. I. (1998), ‘Artificial neural networks for solving ordinary and partial differential equations’, *IEEE transactions on neural networks* **9**, 987–1000.
- Lee, H. & Kang, I. S. (1990), ‘Neural algorithm for solving differential equations’, *Journal of Computational Physics* **91**, 110–131.
- Lewis, A. L. (2016), ‘Option valuation under stochastic volatility II’, *Finance Press* .
- Lord, R., Fang, F., Bervoets, F. & Oosterlee, C. W. (2008), ‘A fast and accurate FFT-based method for pricing early-exercise options under Lévy processes’, *SIAM Journal on Scientific Computing* **30**, 1678–1705.
- Malliaris, M. & Salchenberger, L. (1993), Beating the best: A neural network challenges the Black-Scholes formula, in ‘Proceedings of 9th IEEE Conference on Artificial Intelligence for Applications’, IEEE, pp. 445–449.
- Merton, R. C. (1973), ‘Theory of rational option pricing’, *Bell Journal of Economics and Management Science* **4**, 141–183.
- Merton, R. C. (1976), ‘Option pricing when underlying stock returns are discontinuous’, *Journal of Financial Economics* **3**(1), 125–144.
- Mikhailov, S. & Nögel, U. (2003), ‘Heston’s stochastic volatility model: Implementation, calibration and some extensions’, *Wilmott Magazine* **July**, 74–79.
- O’Sullivan, C. (2005), Path dependant option pricing under Lévy processes, in ‘EFA 2005 Moscow Meetings Paper’.
- Rackauckas, C., Ma, Y., Martensen, J., Warner, C., Zubov, K., Supekar, R., Skinner, D. & Ramadhan, A. (2020), ‘Universal differential equations for scientific machine learning’, *arXiv preprint arXiv:2001.04385* .
- Schmidhuber, J. (2015), ‘Deep learning in neural networks: An overview’, *Neural Networks* **61**, 85–117.

- Sirignano, J. & Spiliopoulos, K. (2018), 'DGM: A deep learning algorithm for solving partial differential equations', *Journal of Computational Physics* **375**, 1339–1364.
- Su, H., Chen, D. & Newton, D. P. (2017), 'Option pricing via QUAD: from Black-Scholes-Merton to Heston with jumps', *Journal of Derivatives* **24**, 9–27.
- Su, H. & Newton, D. P. (2020), 'Widening the range of underlyings for derivatives pricing with QUAD by using finite difference to calculate transition densities - demonstrated for the no-arbitrage SABR model.', *Journal of Derivatives* **28**.
- van Milligen, B. P., Tribaldos, V. & Jiménez, J. (1995), 'Neural network differential equation and plasma equilibrium solver', *Physical Review Letters* **75**, 3594.
- Vasicek, O. (1977), 'An equilibrium characterization of the term structure', *Journal of Financial Economics* **5**, 177–188.
- Yadav, N., Yadav, A. & Kumar, M. (2015), *An introduction to neural network methods for differential equations*, Springer.